Thermal Imidization Behavior of Aromatic Polyimides by Rigid-Body Pendulum Rheometer

Hsien-Tang Chiu, Jui-O Cheng

Graduate School of Polymer Engineering, National Taiwan University of Science and Technology, Taipei 10672, Taiwan

Received 6 September 2007; accepted 28 December 2007
DOI 10.1002/app.27996
Published online 17 March 2008 in Wiley InterScience (www.interscience.wiley.com).

ABSTRACT: Two types of polyamic acid (PAA) precursors were synthesized via combining 3,3′,4,4′-Oxydiphthalicdianhydride (ODPA) with 4,4′-thioetherdianiline (TDA) and 4,4′-sulfonyldianiline (SDA), respectively. Thermal gravity analysis (TGA), rigid-body pendulum rheometer experiment (RPR), and Fourier transform infrared (FTIR) spectroscopy were combined to analyze the thermal imidization processes from precursors PAA to polyimides (PI). This procedure provides the new PAA-PI system with new methods for observing the imidization behavior, thermal properties, and finding the optimization of processing conditions. The results of the TGA and FTIR imidization conversion analysis revealed that the PAA-PI systems synthesized with identical dianhydride and different diamines have distinct reaction temperature regions and reaction speed. The inductive effect of withdrawing and releasing group and the rigidity-flexibility of the molecular chain in the structure of molecular backbone chain influence the imidization reaction. We have seen from the RPR test results that the entire imidization reaction in every isothermal testing temperature reaches an equilibrium condition and completes the gradation reaction of each isothermal temperature within 20 min. Glass transition temperatures (T_g) of PIs increase with increasing the conversion rate from PAA into PI and the rigidity of molecular chain. J Appl Polym Sci 108: 3973–3981, 2008

Key words: polyimides; thermal imidization; glass transition temperature; rigid-body pendulum rheometer; thermogravimetric analysis

INTRODUCTION

Because of the chemical structure found in aromatic polyimides (PI), the backbone chain of polymer has a very high level of rigidity. Since, they have not only excellent thermal stability and flame retardation capability but also good mechanical properties, high chemical and radiation resistance, and low electric constant, they are widely applied in many industries such as aerospace, electrical machinery, precision machinery, cars, electronics, communication, optoelectronics, semiconductors, and so on. Based on the types of processing applications, these materials can be classified into forming/composites materials, injection molding, films, fibers, coatings, foaming formation, enamel-insulated wire, etc.[1]

There are many types of dianhydrides and diamines. The polyimides (PI) with varied properties can be synthesized through different combinations of these components. Therefore, the dehydrated cyclization process will influence the final structure and properties of PI.[2–5] With regard to the new resin system, prior estimations of the processing conditions like curing time and temperature, reaction behavior, conversion degree, etc. are important factors in both research and actual manufacturing applications.

The dynamic mechanical properties of polymer are closely related with its chemical constituents and internal structure.[6]

As regards torsion braid analysis (TBA),[7] mechanical spectrometer (e.g., eccentric rotating disk rheometer, cone and plate rheometer, parallel plates rheometer, concentric cylinders rheometer),[8–15] and rigid-body pendulum rheometer (RPR),[16,17] these kinds of dynamic mechanical analysis (DMA) instruments could be employed for measuring dynamic mechanical properties of melts, fluids, and solids of polymers such as the study of resin-forming reactions and high temperature reactions of thermoplastic polymer. Both of which often start in the liquid state and proceed through gel, rubber, and glassy states.

In applying TBA and mechanical spectrometer to analyze the curing manufacturing properties of paints or resins, the material is placed in an airtight environment to execute the measurement. On the other hand, some of the materials such as paints with solvent content and photocuring resins require to be tested under the open space of removable solvent and illuminated environment. Thus, the application of TBA and mechanical spectrometer in the curing process of the above-mentioned type of mate-

Correspondence to: J.-O. Cheng (d8904008@mail.ntust.edu.tw).

rials is subjected to several limitations. However, a new variation of the DMA apparatus, RPR, developed by Tanaka[16,17] is suitable for testing the curing behavior of these materials in an open environment. Thus it can be said that the RPR can be used in studying the curing process of paints with solvent and photocuring resins.[18,19]

In this study, we combine TGA, RPR, and FTIR to analyze the thermal imidization behavior of PI from the polyamic acid (PAA) precursor, which were synthesized via combining dianhydride-ODPA with two types of diamine-TDA and SDA, respectively. This procedure supplies the new PAA-PI system with new methods for observing its imidization behavior (such as the reaction temperature regions, the reaction time, and the conversion rate) and thermal properties (such as T_g and T_d).

EXPERIMENTAL

Materials and preparation of PAAs

3,3′,4,4′-Oxydiphthalicdianhydride (ODPA) (98Chriskev) was added dividedly several times to a tree-neck flask containing *N,N*-Dimethyl-formamide (DMF) without precipitation in which 4,4′-thioetherdianiline (TDA) (TCI 99% T0632) was previously stirred and dissolved under dry nitrogen gas flow. After the mixture was stirred for 6 h at room temperature, ODPA-TDA PAA 15 wt % in DMF solution was synthesized. The ODPA-SDA (4,4′-sulfonyldianiline) (98Chriskev 44DDS-1000) PAA was also synthesized in DMF solvent using the same procedure as mentioned earlier. Figure 1 shows the preparation of the PAA precursor and polyimide.[20,21]

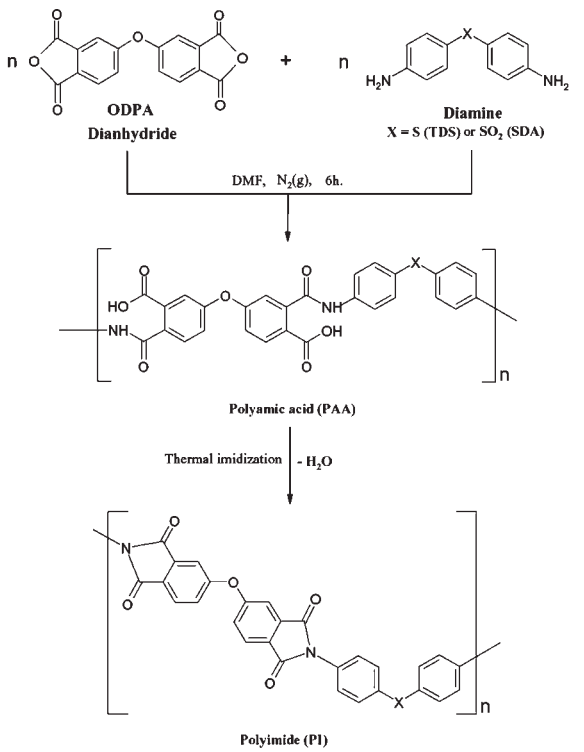

Figure 1 Preparation of polyamic acid (PAA) precursors and polyimides (PI).

Measurement

Thermal gravity analysis

Both ODPA-TDA and ODPA-SDA PAA films were cast from PAAs solution on glass substrate and then proceeding to evaporate DMF at 120°C for 8 h under vacuum. After the PAAs films (thickness of 50 μm) were separated from the glass substrate, the thermal dehydrate imidization temperature zone from PAA to PI and thermal stability of PI was estimated by a thermogravimeter (TA Instruments Q500 type) at a heating rate of 10°C/min under nitrogen.

Fourier transform infrared spectrophotometer

Both ODPA-TDA and ODPA-SDA PAA films were cast from PAAs solution on glass substrate and then isothermally cured at 100, 200, 300, and 350°C for 30 min, respectively. After the PAA films (thickness of 50 μm) were separated from the glass substrate, a Fourier transform infrared (FTIR) spectrophotometer (NEXUS 870 FTIR) was used to measure the imidizated conversion from PAA to PI at a resolution of 2 cm^{-1}.

Rigid-body pendulum rheometer measurement

A RPR (RPT-α 100, Tohoku Electronic Industrial, Japan) with a frame-type pendulum (FRB-300) and knife-edge (RBE-160) was employed to observe the thermal imidization behavior from PAA to PI with isothermal testing at 100, 200, 300, and 350°C for 30 min, respectively. The glass transition temperatures (T_g) of PI after respectively cured at 100, 200, 300, and 350°C for 30 min were investigated by RPR via dynamic scanning testing with 10°C/min of heating rate.

Principle of rigid-body pendulum rheometer

Polymers are examples of viscoelastic materials, which have some of the characteristics of both viscous liquids and elastic solids. Elastic materials have a capacity to store mechanical energy with no dissipation of energy; on the other hand, a viscous fluid in a nonhydrostatic stress state has a capacity for dissipating energy, but none for storing it. When polymeric materials are deformed, part of the energy is stored as potential energy and part is dissipated as

heat. The energy dissipated as heat manifests itself as mechanical damping or internal friction.[6,16–19,22,23]

DMA involves the determination of the dynamic mechanical properties of polymers and their assemblies. As a result of this analysis, the relationship between the dynamic properties and the structural parameters (crystallinity, molecular orientation, molecular weight, crosslinking, copolymerization, plasticization, etc.) and environmental or external variables (temperature, pressure, time, frequency, type of deformation, surrounding atmosphere, humidity, etc.) can be explained.

To determine the dynamic mechanical properties (such as the dynamic modulus E', the loss modulus E'', and the damping or internal friction, tan $\delta = E''/E'$), various vibrational methods are used in nondestructive test. These methods measure the response (deformation) of a material to periodic forces. Thus, the vibrational parameters—amplitude, frequencies, and type of oscillation and wave propagation—become important in this analysis. The physics of vibration and waves has been well developed for these applications.

Four classes of vibrations are often used in the DMA: (1) free vibrations, (2) resonance vibrations, (3) wave propagation, and (4) sinusoidal excitation and response.

At a given frequency of oscillation, the period and the logarithmic decrement define the mechanical behavior of material. This is the underlying principle of all free-vibration experiments. Torsion pendulum, TBA, RPR, etc. were these apparatus which in compliance with the theorem of Free vibrations.

In the RPR experiment, the sample was coated on a plate and fixed on a heating platform. Then, the knife of the pendulum was vertically in contact with sample-coated surface. A schematic diagram of the rigid-body pendulum instrument is shown in Figure 2.

With the application of external force to the pendulum by magnetic adsorption force, the pendulum started a free vibration, and both sides of the knife

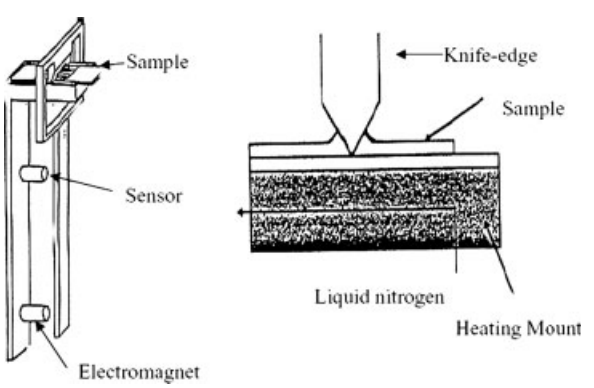

Figure 2 Schematic diagram of the rigid-body pendulum instrument.

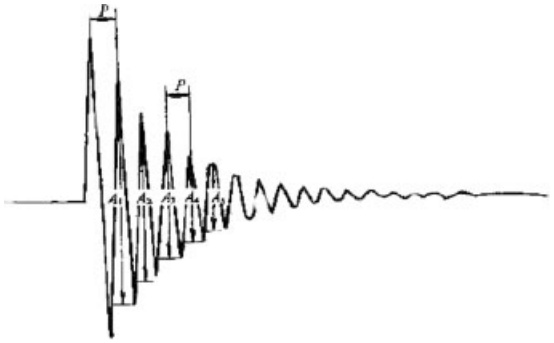

Figure 3 Pendulum displacement-time curve.

of the pendulum gave strains of compression and elongation to the coated test piece. As a result, the viscoelastic property of test pieces created an oscillation period (P) of the pendulum and an oscillatory damping action. The successive amplitudes A_n will decrease with time because of the damping, which gradually converts the mechanical energy of the system into heat. The shear modulus G' is a function of P—the shorter the period, the greater the modulus. By measuring the logarithmic decrement (Δ), the dynamic mechanical properties of sample specimen could be obtained by following eq. (1).

$$\Delta = \ln A_1/A_2 = \ln A_2/A_3 = \cdots\cdots = \ln A_n/A_{n+1} \quad (1)$$

where Δ is the logarithmic decrement or measure of energy dissipation or damping, A_1 is the amplitude of the first oscillation and A_2 is the amplitude of the second oscillation, and that the pendulum displacement-time curve as shown in Figure 3.

RESULTS AND DISCUSSION

Thermal imidization temperature and thermal stability

Under thermal influence, materials generate corresponding transformations with changes in temperature, such as removal of moisture content, evaporation of solvent, degradation and oxidation of material, etc. In the conversion system from PAA into PI, TGA is used to assess and examine the temperature regions of cyclodehydration reaction and the thermal stability and thermal decomposition of PI.

Since the boiling temperature of the solvents containing in PAA are relatively high, the cyclization reaction of PI from precursor PAA involves simultaneous imidization, evaporation of solvent, and crystallization.[2–5,20] To clearly analyze the thermal imidization temperature area, both precursors ODPA-TDA-PAA and ODPA-SDA-PAA were coated into films and vacuum-treated at 120°C for 8 h to remove the solvent before TGA test, which minimizes that

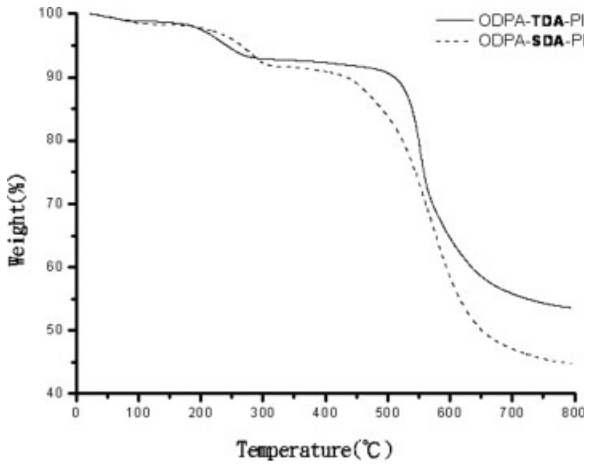

Figure 4 Thermogravimetric analysis of ODPA-**TDA**-PI and ODPA-**SDA**-PI converted from PAA in the dynamic heating testing.

the appearance of thermal imidization temperature areas was overlapped and interfered with the large extent of solvent evaporation in the thermogravimetric analysis.

Figure 4 shows the thermogravimetric analysis of ODPA-TDA-PI and ODPA-SDA-PI converted from PAA in the dynamic heating process. Since the imino group (—NH—) and carboxyl group (—COOH) in the PAA molecular chain easily form hydrogen bonds with water molecules leading to moisture absorption, both the TGA curves show about 1–2% weight loss before 100°C due to the release of adsorptive water molecules and the slight residual solvent. Beyond 100°C, the heat weight loss becomes slighter. At approximately 155°C, the ODPA-TDA curve gradually declines and the beginning of dehydrated cyclization reaction becomes evident. At 300°C, the curve tends to flatten out and the imidization temperature region is found to be at around 155–300°C. On the other hand, ODPA-SDA curve starts to gradually descend when the temperature reaches 176°C and flattens out at around 320°C; the imidization temperature region is at around 176–320°C.

The main cyclodehydration reaction from PAA to PI is regarded as the nucleophilic substitution reaction occuring in itself backbone chain. In the PAA molecular chain, the imino groups (—NH—) are the electron rich reagents to attack the deficient electron of carbon nucleuses in carboxyl group (—COOH) and then substitute the less basicity of hydroxyl group (—OH) to go through nucleophilic substitution reaction.

The imidization reaction speed depend on the steric hindrance, the basicity of imino group (—NH—) or the inductive effect of withdraws or releases electrons in diamine, and the electronic affinity of carboxyl group (—COOH) in dianhydride, etc. The little steric hindrance and the higher basicity of diamine and electronic affinity of dianhydride have the faster imidization rate.[24] Consequently, diamines with electron releasing groups, such as ether (—O—), thioether (—S—), methylene(—CH_2—), enhancing the basicities of imino group that bring faster imidization speed especially when these groups are located at the ortho and para position of the aniline. By contrast, the imidization speed is slower in these diamines with electron withdrawing group like carbonyl (—CO—), sulfonyl (—SO_2—), alkyne, and fluorine contained groups. The thioether (—S—) group of ODPA-TDA-PAA has the less group bulkiness and the inductive effect of electron releasing that strengthens the basicity of imino group (—NH—), and its imidization reaction rate is faster than that of ODPA-SDA-PAA owning the electron withdrawing —SO_2— group. The beginning temperature of the imidization reaction in ODPA-TDA-PAA is at around 155°C, which is quicker than that of ODPA-SDA-PAA at 176°C.

The reaction temperature of the finished imidization is governed by the rigidity-flexibility of the molecular main chain. Main chain segments with higher levels of rigidity have worse chain movability and would require a higher temperature for imidization reaction.[25] Ether (—O—), thioether (—S—), and silicon bonds tend to flexibilize the molecule chain. ODPA-TDA-PAA and ODPA-SDA-PAA were synthesized individually by identical dianhydrides but different diamines. With regard to its molecular chain structure, the diversity between ODPA-TDA-PAA and ODPA-SDA-PAA is in the chain linking segment among the two anilines. The chain linking segment among the two anilines of TDA is thioether (—S—) whose molecular flexibility is greater than the sulfonyl (—SO_2—) chain linking segment in SDA. The finishing imidization temperature of ODPA-SDA is at 320°C which is greater than that of ODPA-TDA at 300°C.

Both curves of ODPA-TDA and ODPA-SDA around 350°C present nearly a flat straight line demonstrating that the imidization reaction is complete at 350°C. The two TGA curves did not drop off until reactions advance upon higher temperature above 350°C. The degradation temperatures (T_d) of weight loss 5% based on 350°C in ODPA-TDA-PI and ODPA-SDA-PI are 529 and 475°C, respectively. The thermogravimetric properties of ODPA-TDA-PI and ODPA-SDA-PI are listed in Table I.

Coversion of isothermal imidization

There are many methods for determining the imidization degree such as the cyclized thermal effect, dielectrics and mechanical loss, nuclear magnetic

TABLE I
The Thermogravimetic Properties of ODPA-TDA-PI and ODPA-SDA-PI

Polyimides	Imidization temperature		5% wt loss T_d based on 350°C	Char yield (%) at 800°C
	Initial	Final		
ODPA-TDA	155	300	529	53.6
ODPA-SDA	176	320	475	44.8

resonance, measurement of the moisture release during cyclization reaction, and estimation of the noncyclized carboxyl group through titration, etc. However, the most widely used method is FTIR.[25]

In the PAA and PI characterization analysis of FTIR, the absorptions at 1550 cm^{-1} (amide I : CNH stretching vibration), at 1660 cm^{-1} (amide II: vibration of C=O in the CONH group), and that in the region 2900–3200 cm^{-1} (amide III: COOH and NH_2 vibration) disappeared after curing. On the other hand, the absorptions at 1780 cm^{-1} (imide I: C=O symmetric stretch), at 1720 cm^{-1} (imide II: C=O asymmetric stretch), at 1380 cm^{-1} (imide III: C—N stretching vibration), and that at 730 cm^{-1} (imide IV: bending vibration of cyclic C=O) appeared after curing.[26–28]

The absorption at 1780 cm^{-1} was the most commonly used value for identifying the imidizated conversion.[29] However, some of the studies indicated that the sensitivities at 1780 and 730 cm^{-1} are lower in the higher imidization conversion[30]; meanwhile, they are interfered with the peak of anhydrides generated in the process. The 1380 cm^{-1} peak was recommended for the determination of imidizated conversion extent.

In this experiment, the adsorption band at 1380 cm^{-1} was monitored during curing from PAA to PI. The adsorption band at 1500 cm^{-1} (C—C stretching of the *p*-substituted benzene) is selected as an internal standard. The conversion to PI during the thermal imidization at temperature T was determined by the following equation[20,21]:

$$\text{Conversion to PI } (\%) = \{(D_{1380\,cm^{-1}}/D_{1500\,cm^{-1}})_T/(D_{1380\,cm^{-1}}/D_{1500\,cm^{-1}})_{350^\circ C}\} \times 100 \quad (2)$$

where D is the optical density of each absorption.

Figure 5 shows the isothermal imidization conversion from both ODPA-TDA and ODPA-SDA PAA into polyimide by FTIR. As the TGA result, both ODPA-TDA-PAA and ODPA-SDA-PAA are almost failed to convert into PI during the isothermal curing at 100°C. The conversion to PI increases with increasing the curing temperature. The imidization speed of ODPA-TDA-PAA is faster than ODPA-SDA-PAA. Therefore, the conversion of ODPA-TDA-PI from PAA is greater than ODPA-SDA-PI at the isothermal curing of 200°C at 31.53 and 21.41%, respectively. At the isothermal curing of 300°C, the two imidization conversions reached 90% and above. At this reaction stage, the conversion rate is obviously high.

Imidization behavior and glass transition temperature

The thermal curing process involves the simultaneous cyclization with dehydration, evaporation of solvent, and crystallization, so it will influence the final structure and properties of polyimide. To observe and control the final properties of PI, it is essential to analyze the imidization process in detail.

The imidization behaviors from ODPA-TDA and ODPA-SDA PAA to polyimide were observed with respectively isothermal curing at 100, 200, 300, and 350°C for 30 min by RPR.

The imdization behaviors of isothermal curing of ODPA-TDA PAA to PI are shown in Figure 6. As the time of isothermal test increases, the simultaneous cyclization with dehydration and evaporation of solvent gradually increase which bring an increase in viscosity of the sample specimens. In about 1.5 min of test time, the four RPR curves of isothermal reaction in the illustration start to rise with the swift increase in viscosity of the sample specimens.

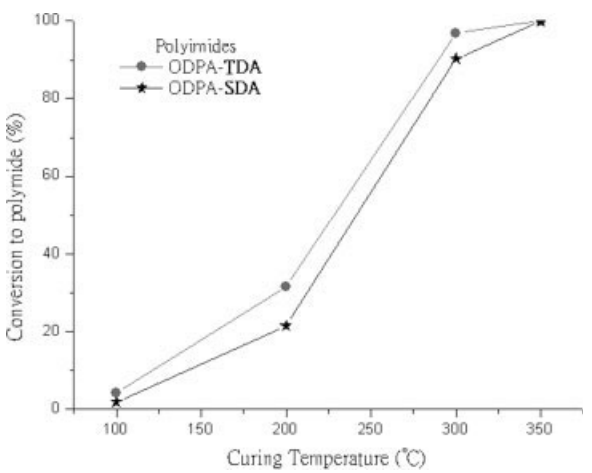

Figure 5 The isothermal imidization conversion from both ODPA-**TDA** and ODPA-**SDA** polyamic acid into polyimide by FTIR.

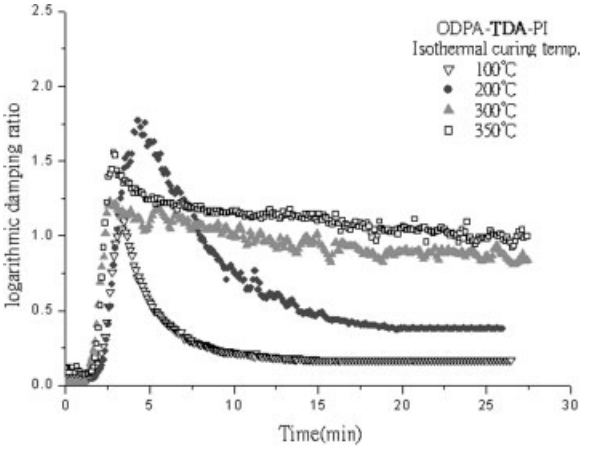

Figure 6 The imidization behavior from ODPA-**TDA** polyamic acid to polyimide with four isothermal curing by RPR.

This turning point is called gel point and the corresponding time is called gel time. In a complicated curing reaction such as the imidization process, various overlapping phenomena can occur in the same temperature region. The overall reaction of the four sample specimens reached the equilibrium condition within 20 min, completing the gradation reaction of each isothermal test temperature.

Some studies indicate that the thermal imidization process of solid state PAA usually has two stages, i.e., the fast stage followed by the slow stage. Under a fixed temperature, imidization slows down and eventually stops after it reaches a certain reaction conversion degree. When the temperature is increased, it will react immediately. However, it will slow down again after a few minutes until the temperature is increased to the point when imidization is completed. That is to say, the imidization reaction in the solid state depends on the temperature and has very little relation with time. When the imidization reaction speed slows down under a certain temperature so that it gets close to nil, this phenomenon is called ''kinetics discontinuance.''[31–34]

Based on the TGA and FTIR analyses results, we know that the imidization reaction in the isothermal curing of 100°C has not almost started yet. The RPR curve of isothermal 100°C shows that a gradual descent to a low equilibrium value after the damping rises to a high point as it passes through solvent evaporation.

From each isothermal curing curve of RPR, we can observe a relationship between the damping altitude of reaction equilibrium and the conversion degree of imidization. When the imidization conversion degree is higher, the skeletal structure of PI is much more rigid compared to that of PAA because of cyclization,[20] and the damping altitude of reaction equilibrium is also higher. In the previous FTIR results, the conversion rate at 300°C isothermal curing reached 96.85%. In the RPR isothermal reaction curve, the reaction equilibrium altitude of 300°C curve was considerably close to that of the 350°C curve. This means that the imidization is gradually tended to complete at 300°C isothermal curing.

Figure 7 shows the imidization behavior from ODPA-SDA PAA to polyimide with four isothermal curing by RPR. The ODPA-SDA PAA reaction curves also present similar ODPA-TDA tendency as mentioned earlier. In about 1.8 min of test time, the four RPR curves of isothermal reaction in the illustration start to rise with the swift increase in viscosity of the sample specimens, while the total reaction was completed within 20 min. As the imidization conversion degree goes higher, the equilibrium altitude of the reaction curve is also higher while the reaction equilibrium altitude of the 300°C curve gradually approaches that of the 350°C curve.

Figure 8 shows the comparison of imidization behavior between the ODPA-TDA and ODPA-SDA cured from PAA into polyimide at 350°C isothermal curing by RPR. The illustration revealed that the rigidity of molecular chain affects the last damping altitude of reaction equilibrium. Since the flexibility of —S— linkage in the molecular chain of ODPA-TDA-PI is greater than the —SO_2— linkage in ODPA-SDA-PI, the —S— linkage of TDA was easier to bend or move than the —SO_2— linkage of SDA. The final equilibrium damping altitude of ODPA-TDA-PI was lower than that of ODPA-SDA-PI.

To further understand the imidization conversion condition after various isothermal curing processes, the imidization curing of ODPA-TDA-PAA and ODPA-SDA-PAA were performed in advance at isothermal 100, 200, 300, and 350°C for 30 min on the RPR heating platform. Then, the dynamic scanning testing of RPR was employed to examine the molec-

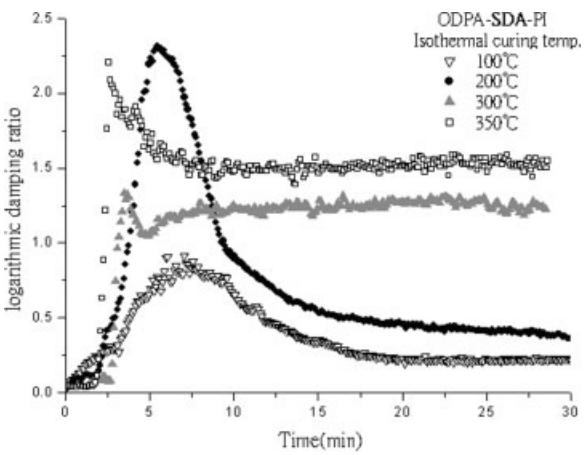

Figure 7 The imidization behavior from ODPA-**SDA** polyamic acid to polyimide with four isothermal curing by RPR.

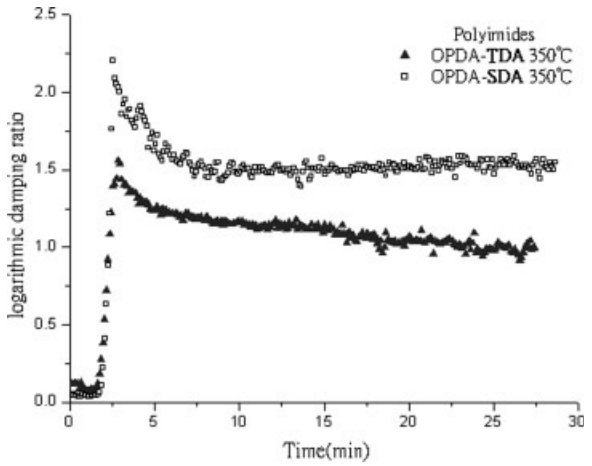

Figure 8 The comparison of imidization behavior between the ODPA-**TDA** and ODPA-**SDA** cured from polyamic acid into polyimide at 350°C isothermal curing by RPR.

ular chain motion temperatures (T_g) of PI with different conversion degrees.

Values of T_g depend on the chemical structure. Flexibility of the molecular chain depends on the free-volume theory, and thermodynamic theory is one of the factors to influence the value of T_g.[35,36]

The dynamic scanning curves of ODPA-TDA-PI after converted from PAA with four isothermal curing are shown in Figure 9. Based on the analysis results of TGA, FTIR, and isothermal curing of RPR, we found that the imidization reaction at the isothermal curing of 100°C did not really start and its isothermal temperature was much lower than the boiling point (153°C) of PAAs DMF solvent. For 30 min under an isothermal 100°C curing without vacuum treatment, the sample system still contained considerable quantities of remnant solvent. Figure 9 reveals that during the dynamic scanning testing with a heating rate of 10°C/min, the dynamic scanning curve of ODPA-TDA-PI cured in advance with isothermal 100°C begins to proceed with simultaneous evaporation of the residual solvent and follow-up cyclization reaction at around 120°C. Following this progress of dynamic heating cyclization process, the degree of imidization conversion gradually increases. In conclusion, the ultimate appearance of T_g peak of the molecular chain is at 276°C.

Isothermal curing at 200°C has partial imidization reaction. Partially cured is regarded as PAA-PI random copolymer.[20] In the dynamic scanning curve of 200°C isothermal curing of sample specimen, since the cyclization conversion is smaller and the free volume (V_f) of molecular chain is bigger, some of the molecular chain segments continuously initiate movements at around 181°C of lower temperature regions. The T_g peak temperature at the specimen with 200°C isothermal curing is 250°C, which is lower compared to T_g peak temperatures of the specimens with 300 and 350°C isothermal curing. The kinetics discontinuance phenomenon, in which the imidization reaction slows down and eventually stops after it reaches a certain reaction conversion degree under a fixed temperature, is generally believed that the movability of molecular chains appear changes during the reaction process. As soon as the imidization reaches a certain conversion degree during the cyclization process, the vitrified temperature of polymer enhances. The polymer becomes glassy from rubbery and the motion of molecular chain is hindered or frozen so that it becomes difficult to proceed to further imidization process. The retardation in cyclization speed is due to the decrease in the movability of molecular backbone chain.[37] The temperature must be raised over T_g so that the thermal energy is sufficient to surmount the potential barriers for translational and rotational

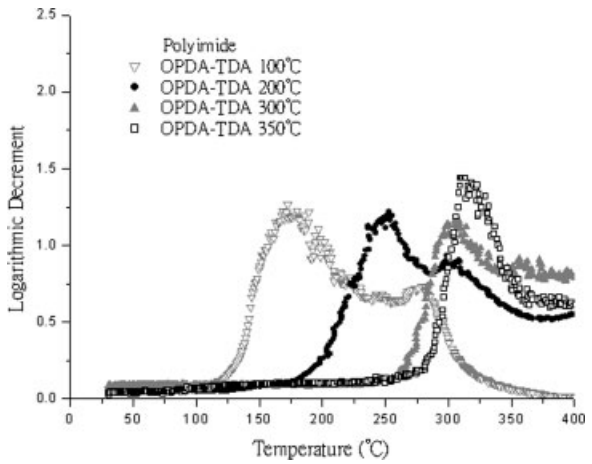

Figure 9 The dynamic scanning curves of ODPA-**TDA**-PI after converted from PAA with four isothermal curing.

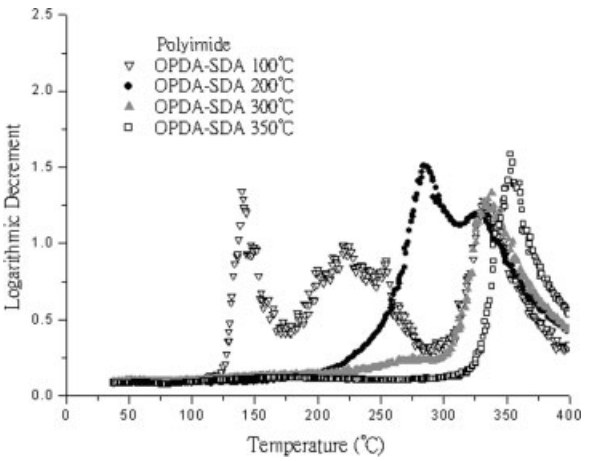

Figure 10 The dynamic scanning curves of ODPA-**SDA**-PI after converted in advance from PAA with four isothermal curing.

TABLE II
The T_g Peak Values of the Dynamic Scanning Curves of ODPA-TDA-PI and ODPA-SDA-PI in Figures 9 and 10

	Isothermal 100°C			Isothermal 200°C		Isothermal	Isothermal
Polyimides	Peak 1	Peak 2	Peak 3	Peak 1	Peak 2	300°C	350°C
ODPA-TDA	173°C	276°C		250°C	301°C	303°C	317°C
ODPA-SDA	139°C	223°C	330°C	288°C	330°C	334°C	353°C

motions of segments of the polymer molecules. The reaction will initiate again and proceed speedy that will serve to elevate the imidization conversion. Following the 250°C T_g peak in the specimen with 200°C isothermal curing, more remnant reactions continuously progress because the temperature is raised continuously to devitrify.[38] Since the cyclodehydration reaction continuously produce by-product such as water, which causes an increase in energy dissipation. Therefore, the damping curve of dynamic scanning beyond the 250°C of Tg peak yields an increase in small peaks in the 276–350°C range, after which damping gradually drops off.

When the imidization degree increases during the conversion of PAA to PI, the quantities of molecular side chains like the —OH of —COOH and the —H of —NH— are gradually reduced bringing the decrement of movable V_f in the molecular end chain group. The skeletal chain becomes more rigid causing the T_g to increase and shift to a higher temperature region. Figure 9 reveals that because the imidization conversion is high in the specimens with 300 and 350°C isothermal curing, the damping curves shows only one peak which is not succeeded by any reaction. Their T_g peak temperatures are 303 and 317°C, respectively, and both T_g are relatively near to each other which signifies that conversion reaction is almost completed.

Figure 10 shows the dynamic scanning curves of ODPA-SDA-PI after converted from PAA with four isothermal curing. The same phenomenon as the above-mentioned ODPA-TDA is seen from the dynamic scanning curve of ODPA-SDA-PI where the thermal imidization reaction has not nearly began at isothermal 100°C curing, and the sample specimen still contains a large amount of residual solvent. At approximately 120°C, the processing involves simultaneous evaporation of residual solvent and follow-up cyclization reaction begins to proceed, and finally, the ultimate appearance of T_g peak of the molecular chain is at 330°C. Isothermal curing at 200°C has partial imidization conversion. Some of the molecular chain segments initiate the movements at around 201°C of lower temperature regions. The T_g peak temperature of the specimen with 200°C isothermal curing is at 288°C, which is lower than the T_g peak temperatures of the specimens with 300 and 350°C isothermal curing. Following the 288°C of T_g peak in the specimen with 200°C isothermal curing, the continuous increase in temperature causes more remnant reactions to proceed. Therefore, the damping curve beyond the 288°C of T_g peak shows an increase in small speaks among 313–360°C, after which the damping curve gradually drops off.

The T_g of PAA increases along with the conversion to PI by thermal curing. Imidization degrees in the specimens with 300 and 350°C isothermal curing are relatively high. Damping curves present only a single peak which is not succeeded by any other reaction. Their T_g peak temperatures are 334 and 353°C, respectively, and both T_g are fairly near each other, which means that the conversion reaction is almost completed. The T_g peak values of the dynamic scanning curves of ODPA-TDA-PI and ODPA-SDA-PI in Figures 9 and 10 are listed in Table II.

Figure 11 shows the comparison of the glass transition temperature between ODPA-TDA-PI and ODPA-SDA-PI converted from PAA with 350°C isothermal curing. Values of T_g depend on the chemical structure. Flexibility of the molecular chain is one of the factors that affect the value of T_g. The thioether (—S—) linkage segments of ODPA-TDA-PI molecular chain tend to cause chain flexibility, and its flexibility proved larger than the —SO_2— linkage segments of ODPA-SDA-PI. The —S— linkage of TDA was easier to bend or move than the —SO_2— linkage

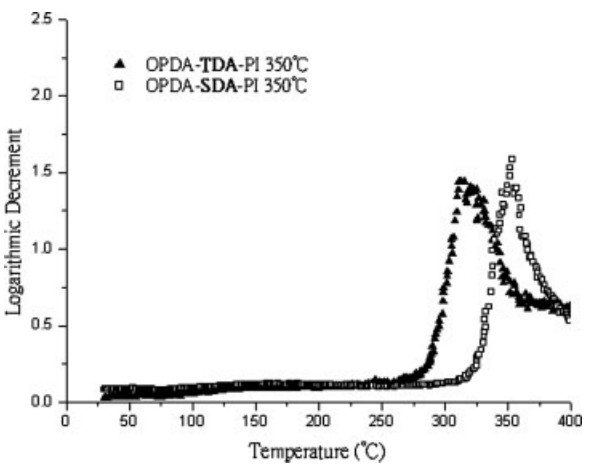

Figure 11 The comparison of glass transition temperature between ODPA-**TDA**-PI and ODPA-**SDA**-PI converted from PAA with 350°C isothermal curing.

of SDA. As a result, the T_g (317°C) of ODPA-TDA-PI is lower than the T_g (353°C) of ODPA-SDA-PI.

CONCLUSION

The TGA results reveal that the PAA-PI systems synthesized by identical dianhydride with different diamines have distinct reaction temperature regions and reaction speeds. The inductive effect of withdrawing and releasing group and the rigidity-flexibility of the molecular chain in the structure of molecular backbone chain influence the reaction movement. The thioether group (—S—) of ODPA-TDA-PAA has the inductive effect of releasing electron effects that strengthen the basicity of imino groups (—NH—), and its imidization reaction rate is faster than that of ODPA-SDA-PAA with —SO_2— of withdrawing electrons group. The thioether (—S—) chain linking segment among two anilines of TDA has greater molecular flexibility than the —SO_2— chain linking segment in SDA. The complete imidization temperature of ODPA-TDA is lower than ODPA-SDA.

The FTIR imidization conversion analysis results show that the imidization speed of ODPA-TDA-PAA is faster than that of ODPA-SDA-PAA.

As seen in the results derived from the RPR tests, the total imidization reaction in each isothermal temperature reaches equilibrium within 20 min and completes the gradation reaction of each isothermal test temperature. The damping altitude of isothermal curing equilibrium reaction and T_g are closely related to the degree of imidization conversion. Upon increasing the conversion from PAA into PI, the skeletal structure of PI is much more rigid compared with that of PAA because of cyclization while the reaction equilibrium damping altitude and T_g are found to increase likewise. That is to say, the rigidity of the molecular chain affects the final reaction equilibrium damping altitude and T_g. In the molecular structure of ODPA-TDA-PI, the flexibility of thioether (—S—) linkage is greater than the sulfonyl (—SO_2—) linkage in ODPA-SDA-PI. Therefore, the final damping altitude of reaction equilibrium and T_g of ODPA-TDA-PI are lower than ODPA-SDA-PI.

The result of the combined use of TGA, FTIR, and RPR showed a high degree of correlation between the thermomechanical and thermal spectra of the polymers. With regard to the thermal imidization process, the analysis provided good estimation methods of the processing conditions (e.g., curing time and temperature, reaction behavior, conversion degree, etc.). They are useful in both research and actual industry manufacturing applications in terms of observing and controlling the final properties of PI and in reducing the manufacturing costs (e.g., capacity of equipment, energy resources, operation time, etc.).

References

1. Lin, C. C.; Chen S. M. Applications and Technology Development Trends in Polyimides; ITRI: Taiwan, 1999; Chapter 1–2.
2. Kim, H. T.; Park, J. K. Polym J 1997, 29, 1002.
3. Ojeda, J. R.; Mobley, J.; Martin, D. C. J Polym Sci Part B: Polym Phys 1995, 33, 559.
4. Miwa, T.; Okabe, Y.; Ishida, M. Polymer 1997, 38, 4945.
5. Stoffel, N. C.; Kramer, E. J.; Volksen, W.; Russell, T. P. Polymer 1993, 34, 4524.
6. Murayama, T. Dynamic Mechanical Analysis of Polymer Material; Elsevier: New York, 1978; Chapter 1–2.
7. Gillham, J. K. Techniques and Methods of Polymer Evaluation; Marcel Dekker: New York, 1970; p 225.
8. Harris, J.; Wilkinson, W. L. Br Soc Rheol Bull 1969, 1, 1.
9. Walters, K.; Kemp, R. A. Rheologica Acta 1968, 7, 340
10. Warburton, B.; Davis, S. S. Rheologica Acta 1969, 8, 205.
11. Macosko, C. W.; Starita, J. M. SPE J 1971, 27, 38.
12. Macosko, C. W.; Weisset, F. C. American Society for Testing and Materials, Spec Tech Publ No 553, Philadelphia, PA, 1974.
13. Davis, W. M.; Macosko, C. W. AIChE J 1974, 20, 600.
14. Broyer, E.; Macosko, C. W. SPE ANTEC 1975, 21, 343.
15. Davis, W. M.; Macosko, C. W. SPE ANTEC 1976, 22, 408.
16. Tanaka, T. Coating Films Evaluation of Physical Property; Ricogaka: Japan, 1993.
17. Tanaka, T. Proceedings of the International Pressure Sensitive Adhesive Technoforum; Tokyo, Japan, 1997.
18. Chiu, H. T.; Wu, J. H. J Appl Polym Sci 2005, 97, 711.
19. Chiu, H. T.; Wu, J. H. Polym Plast Technol Eng 2006, 45, 1081.
20. Kotera, M.; Nishino, T. K.; Nakamae, K. Polymer 2000, 41, 3615.
21. Nishino, T.; Kotera, M.; Inayoshi, N.; Miki, N.; Nakamae, K. Polymer 2000, 41, 6913.
22. Chiu, H. T.; Wu, J. H. J Polym Res 2004, 11, 247.
23. Chiu, H. T.; Wu, J. H. J Appl Polym Sci 2005, 98, 1206.
24. Kolegov, V. I.; Sklizkova, V. P.; Kudriavtsev, V. V.; Belen'kii, B. G.; Frenkel, S. Y.; Koton, M. M. Dokl Akad Nauk SSSR 1977, 232, 848.
25. Ting, M. H.; Ho, T. P. New Type Material—Polyimides; Science Pub.: Beijing, 1998; Chapter 1.
26. Pryde, C. A. J Polym Sci Part A: Polym Chem 1989, 27, 711
27. Nah, C.; Han, S. H.; Lee, J. H.; Lee, M. H.; Lim, S. D.; Rhee, J. M. Compos Part B: Eng 2004, 35, 125.
28. Jordan, K.; Iroh, J. O. Polym Eng Sci 1996, 36, 2550.
29. Ginsberg, R.; Susko, J. R. In Polymides: Synthesis, Characterization and Properties; Mittal, K. L., Ed.; Plenum: New York, 1984; Vol. 1, p 237.
30. Navarre, M. In Polyimides: Synthesis, Characterization and Properties; Mittal, K. L., Ed.; Plenum: New York, 1984; Vol. 1, p 259.
31. Laiua, L. A.; Tsapovetskii, M. I. In Polyimides: Synthesis and Characterization; Mittal, K. L., Ed.; Plenum: New York, 1984; Vol. 1, p 295.
32. Sememova, L. S.; Lishansky, I. S.; Illarionova, N. G.; Michailova, N. V. Vysokomol Soedin 1984, 26, 1809.
33. Kardash, L. E.; Ardashnikov, A. Y.; Yakushin, F. S.; Pravdnikov, A. N. Vysokomol Soedin 1975, 17, 598.
34. Seo, Y. Polym Eng Sci 1997, 37, 772.
35. Nielsen, L. E. Mechanical Properties of Polymers and Composites; Marcel Dekker: New York, 1974.
36. Aklonis, J. J.; Macknight, W. J.; Shen, M. Introduction to Polymer Viscoelasticity; Wiley: New York, 1972.
37. Koton, M. M.; Meleshko, T. K.; Kudriavtsev, V. V.; Nechayev, P. P.; Kamzolkina, Y. V.; Bogorad, N. N. Vysokomol Soedin 1982, 24, 791.
38. Chiu, H. T.; Jeng, R. E.; Chung, J. S. J Appl Polym Sci 2004, 91, 1041.